New Observational Views on the Chemistry of Diffuse Interstellar Clouds

Helmut Wiesemeyer
MPIfR Bonn
SOFIA Community Tele Talk 2018 June 27

Collaborators:

R. Güsten, K.M. Menten, J. Stutzki, T. Csengeri, C. Durán, H.W. Hübers, A.M. Jacob, B. Klein, D.A. Neufeld, H. Richter, O. Ricken, C. Risacher, R. Simon, B. Winkel, F. Wyrowski

Acknowledgements:

SOFIA telescope and mission support,
insightful discussions with M. Gerin and P. Goldsmith

Overview

- Introduction: Phases of the ISM, diffuse gas characteristics, reaction kinetics.
- Diffuse gas tracers, observational techniques, quantitative analysis.
- Putting it all together: Chemical reaction networks and observed abundances.
- Towards a more realistic -and complex- picture

Phases of the ISM

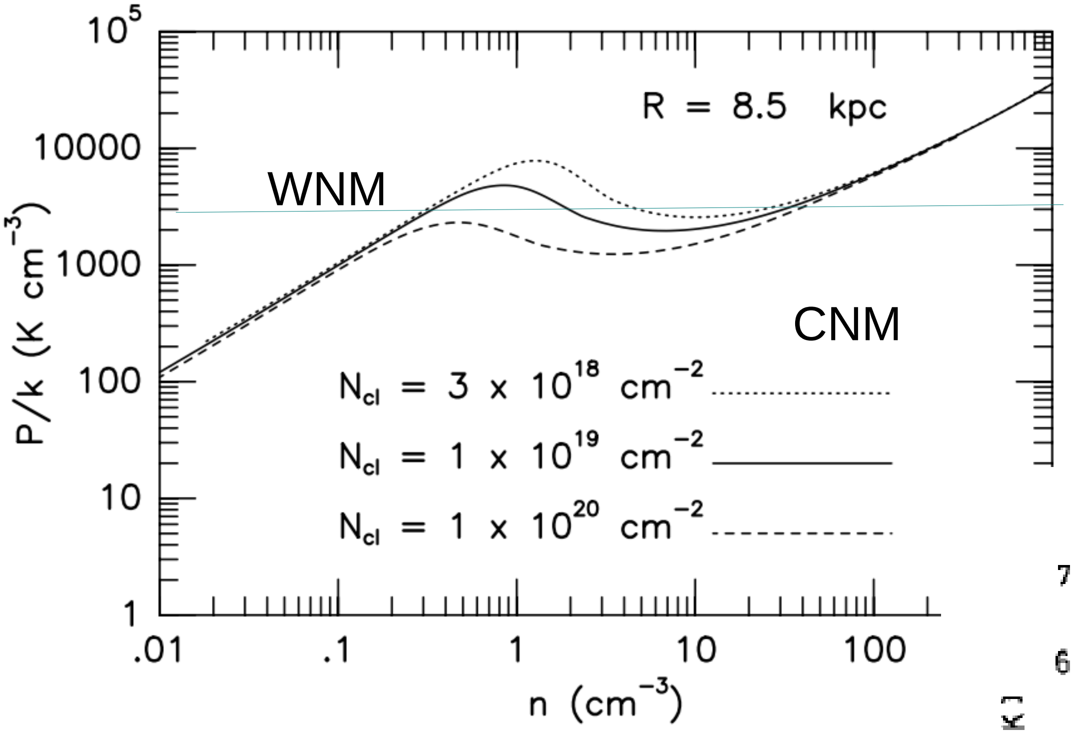

← Wolfire et al., 2003

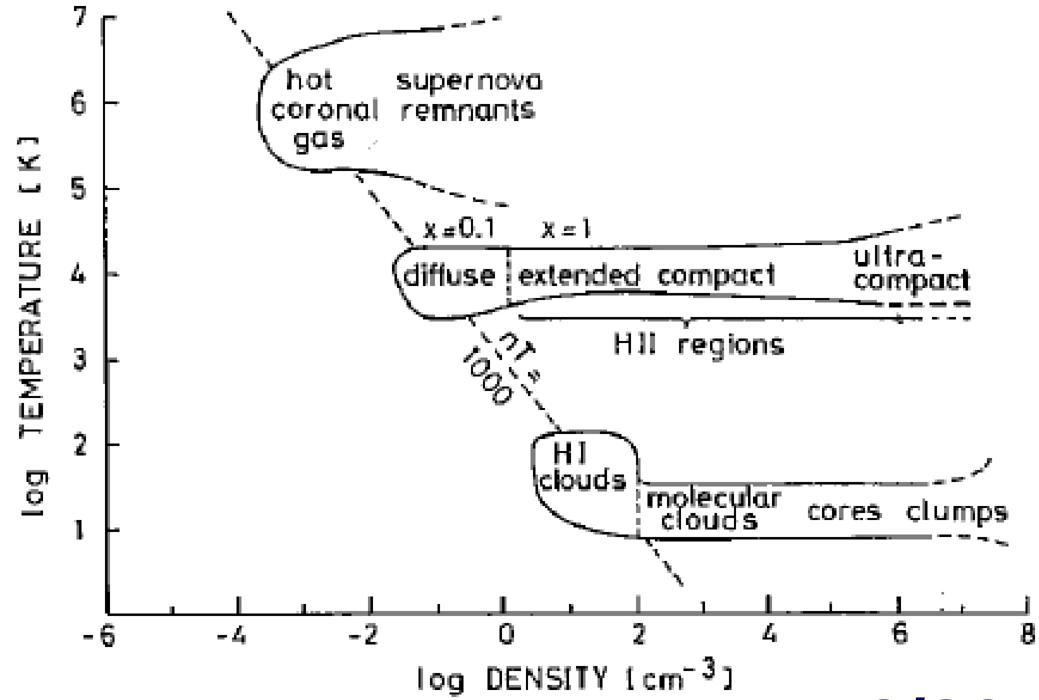

Yorke, Saas-Fee Lecture 1988 →

Characteristics of interstellar clouds

	Diffuse Atomic	Diffuse Molecular	Translucent	Dense Molecular
Definition	$f^n_{H2} < 0.1$	$f^nH_2 > 0.1$ $f^n_{C^+} > 0.5$	$f^n_{C+} < 0.5$ $f^n_{CO} < 0.9$	$f^n_{CO} > 0.9$
$A_v >$	0	~ 0.2	~ 1 – 2	~ 5 - 10
n_H ~ [cm^{-3}]	10 - 100	100 - 500	500 - 5000	> 10^4
T_{gas} [K]	30 - 100	30 - 100	15 – 50 ?	10 - 50
Technique	UV/Vis abs., HI λ21cm	UV to mm abs, radio abs/em.		IR absorption, FIR to radio em.

Freely adapted from Snow & McCall 2006, ARA&A 44.

Characteristics of interstellar clouds

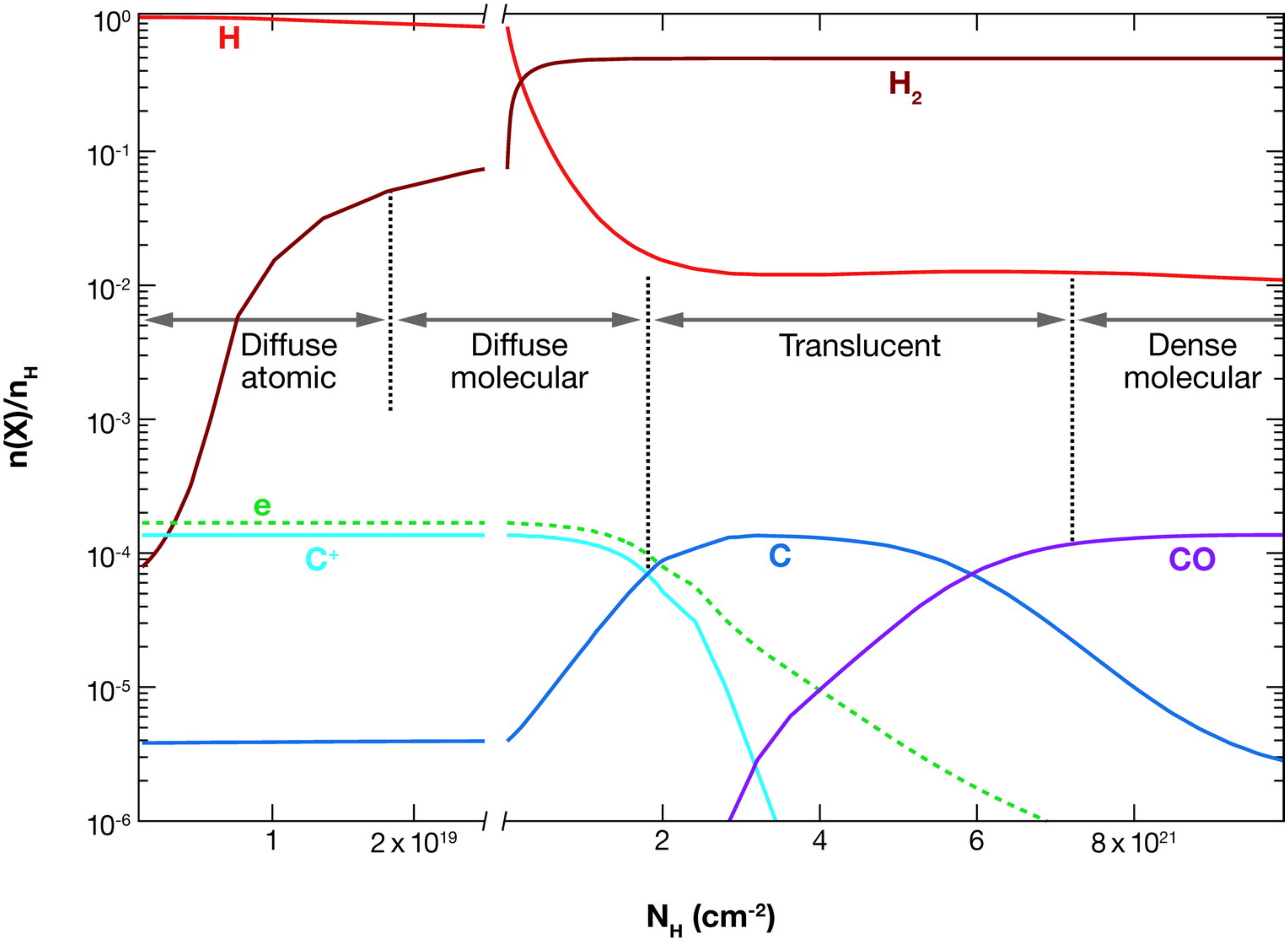

Snow TP, McCall BJ. 2006.
Annu. Rev. Astron. Astrophys. 44:367–414

Reaction kinetics

Element	Ionization potential (eV)	Endothermicity (Kelvin equivalent = $\Delta E/k_B$) for			Driver
		$X + H_2 \rightarrow XH + H$	$X^+ + H_2 \rightarrow XH^+ + H$	$X + H_3^+ \rightarrow XH^+ + H_2$	
He	24.587	No reaction	Exothermic, but primary channel is to $He + H + H^+$	29,000	
C	11.260	11,000	4,300 ✓		Warm gas
N	14.534	15,000	230	10,000	Cosmic rays
O	13.618	920 ✓	✓	✓	Warm gas or cosmic rays
F	17.423	✓		10,000	None needed
Ne	21.564	No reaction	Exothermic, but primary channel is to $Ne + H + H^+$	27,000	
Si	8.152	17,000	15,000		Warm gas
P	10.487	19,000	13,000		Warm gas
S	10.360	10,000	10,000 ✓		Warm gas
Cl	12.968	515	✓		UV with $h\nu > 12.97$ eV
Ar	15.760	No reaction	✓	6,400	Cosmic rays

Gerin M, et al. 2016.
Annu. Rev. Astron. Astrophys. 54:181–225

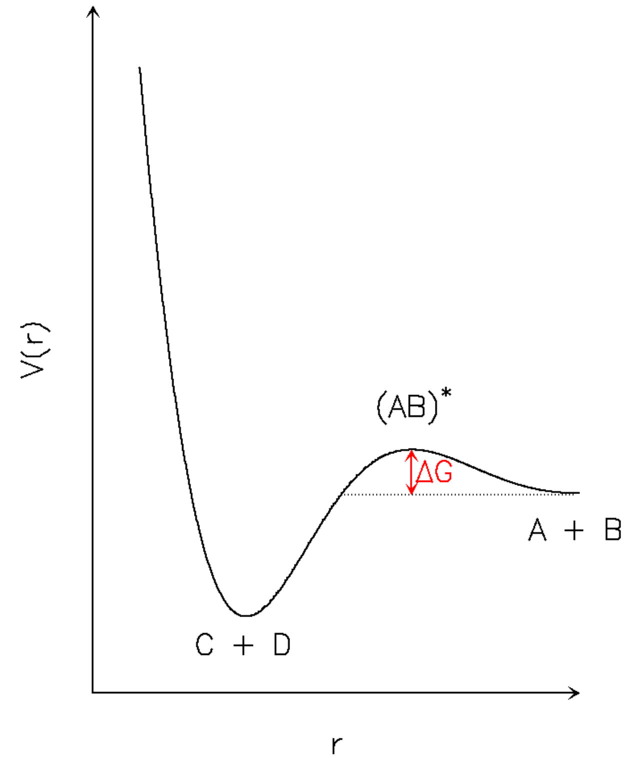

Potential energy curve for an exothermic reaction with activation energy ΔG

- exothermic
- endothermic
- weakly endothermic ($\Delta E/k_B \sim 1000$ K)

Observational techniques:
Absorption spectroscopy towards bright background sources

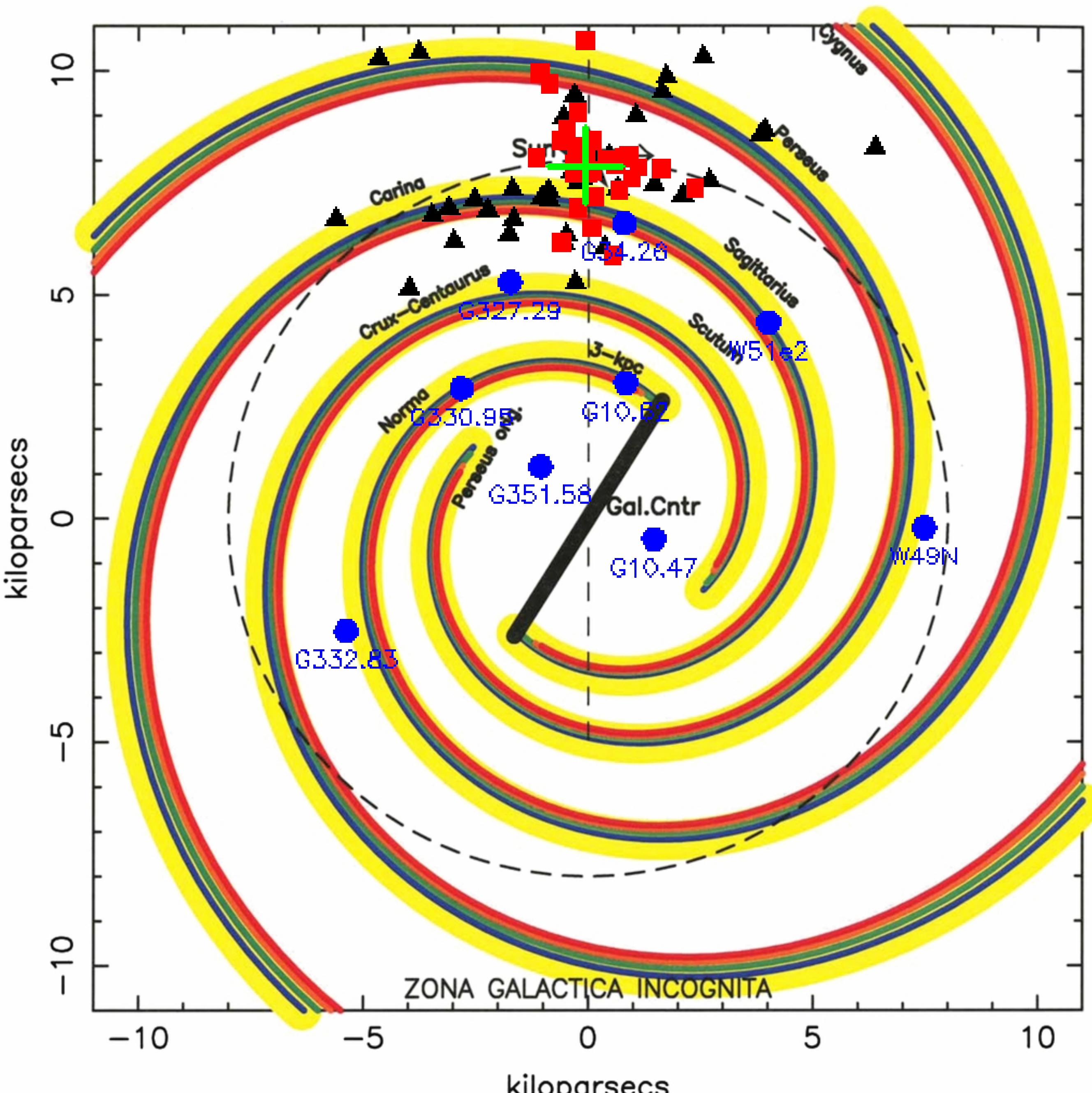

Galactography from Vallée (2014)

▲ Sheffer et al. (2008), far-UV (H_2)/optical (CH)

■ Jensen et al. (2005), UV (OI)

● Wiesemeyer et al. (2016, 2018), FIR: OI, OH, OH^+, CH, distances: Reid ea. 2014

Observational Techniques:
UV/optical vs. FIR/submm absorption

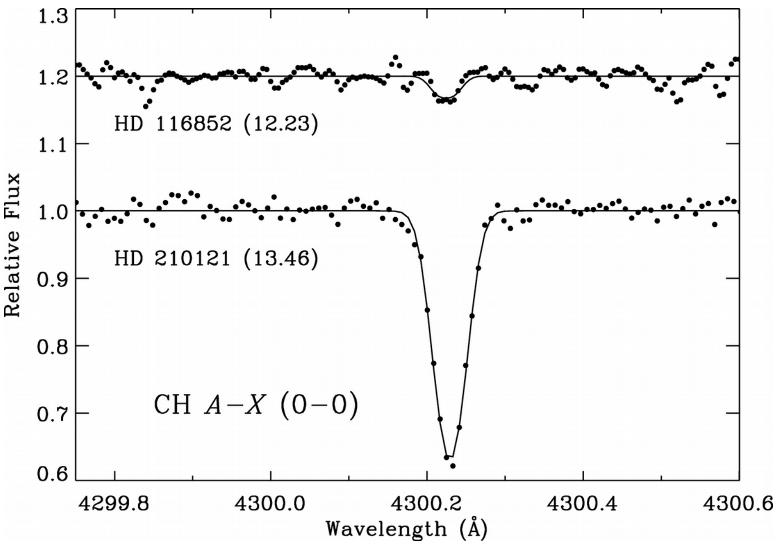

Optical sample spectrum of CH A-X (0-0), λ4300Å, velocity resolution 1.8 km/s (Sheffer et al. 2008)

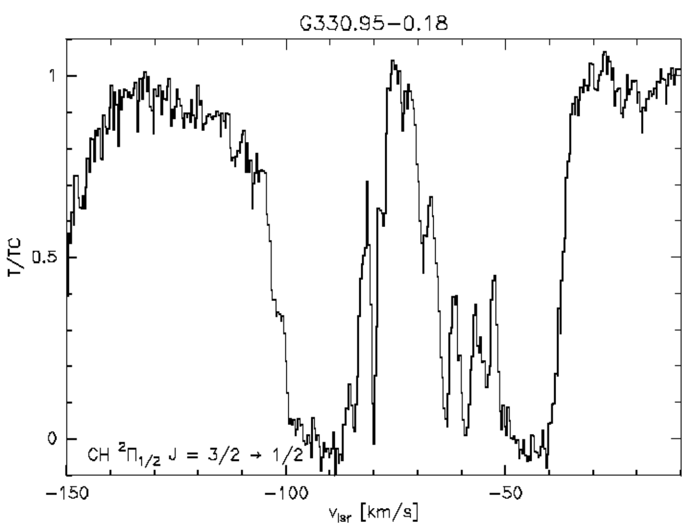

Far-infrared sample spectrum of CH $^2\Pi_{1.2}$ J = 3/2 ←1/2, λ149 μm, velocity resolution 0.3 km/s (smoothed, Wiesemeyer et al. 2018)

UV/Optical Spectroscopy

- Restricted to local arm
± a few kpc.
- Examination of sightlines off the Galactic plane.
- Spectral resolution:
FUSE: R ~ 10^4, HST-STIS:
R ~ 6×10^4, optical: R ~ $1.7\ 10^5$
- Needs excitation modeling and extinction corrections.

FIR Spectroscopy

- Does not suffer from extinction (but absorption may saturate).
- Restricted to FIR-bright targets (hot dust from star forming regions)
- Spectral resolution: R ~ 10^7 (upGREAT, LFA)
- Ground state transitions,,
no extinction corrections needed:

$$\tau_{\mathrm{ij},\upsilon} = \sqrt{\frac{\ln 2}{\pi}} \frac{A_{\mathrm{E},j} c^3}{4\pi \Delta\upsilon_{\mathrm{i}} \nu_{\mathrm{j}}^3} \frac{g_{\mathrm{u,j}}}{g_{\mathrm{l,j}}} N w_{\mathrm{j}} \exp\left(-4\ln 2 \left(\frac{\upsilon - \upsilon_{0,ij}}{\Delta\upsilon_i}\right)^2\right),$$

Quantitative Analysis: Surrogates for H_2

Primary tracers:

- FIR ground-state lines of HF, OH, CHl H_2O
- HF, OH and H_2O saturate frequently.
- CH and OH do not necessarily trace the same environment, but are correlated.
- The λ63 μm fine structure line of [OI] traces the hydrogen reservoir $2N(H_2)+N(HI)$

Secondary tracers:

- Radio lines of OH and CH.
- HCO^+ $J = 1 \leftarrow 0$ (correlates with OH, Liszt & Lucas 1996),
- Some hyperfine components of OH and CH appear in emission and absorption.
- Also probe physical conditions (n, T), not just column density, but collisional rates uncertain.

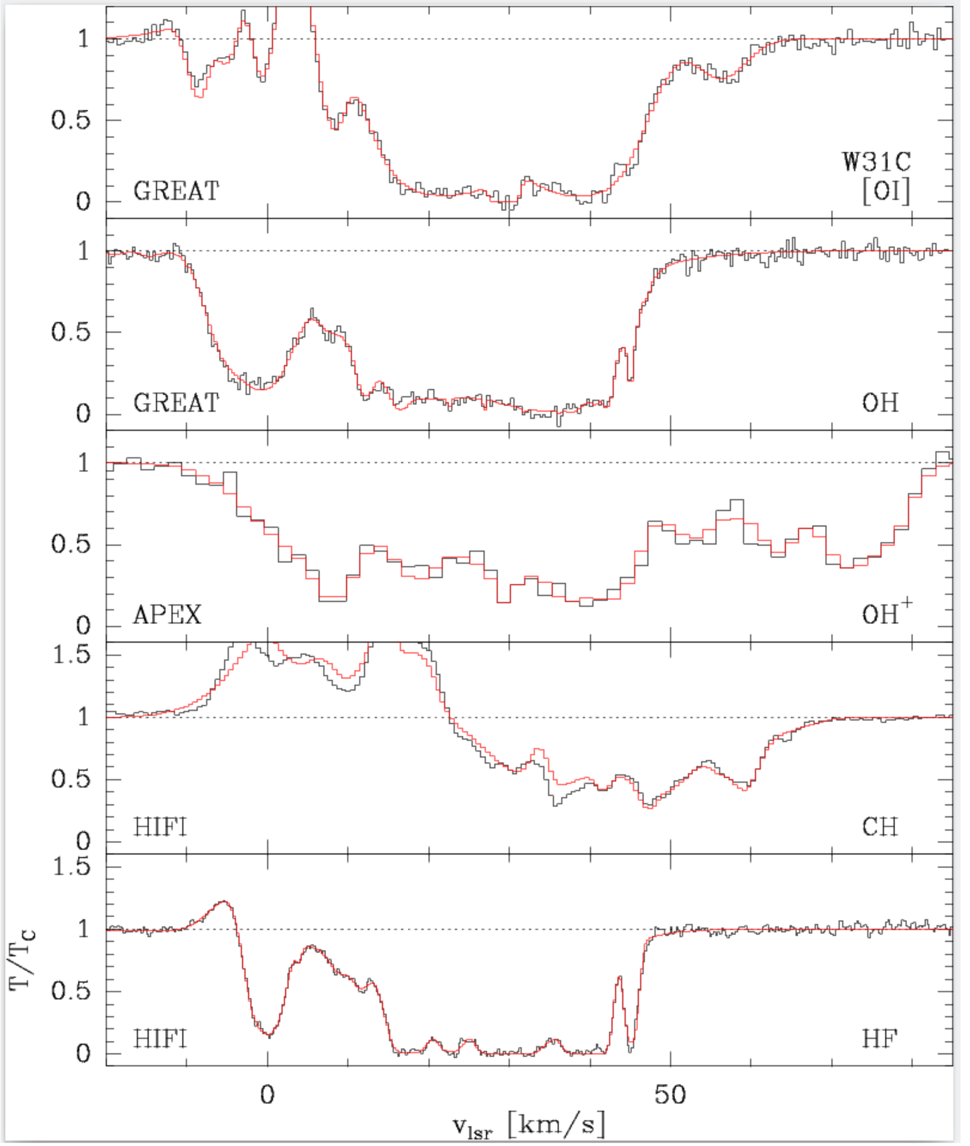

Wiesemeyer et al. (2016)

Quantitative analysis: Devonvolution from hyperfine structure and component separation

- The blend between hyperfine structure and overlapping velocity components requires a deconvolution strategy, like
- “Shift and subtract” (e.g., Gerin et al. 2010),
- principal component analysis (e.g., Neufeld et al. 2015 → et al. 2018 in prep.),
- Wiener-filter deconvolution (Jacob et al. 2018 in preparation),
- merit function minimization, e.g., Levenberg-Marquardt optimization (Schilke et al. 2001), simulated annealing (e.g., Wiesemeyer et al. 2016, 2018).

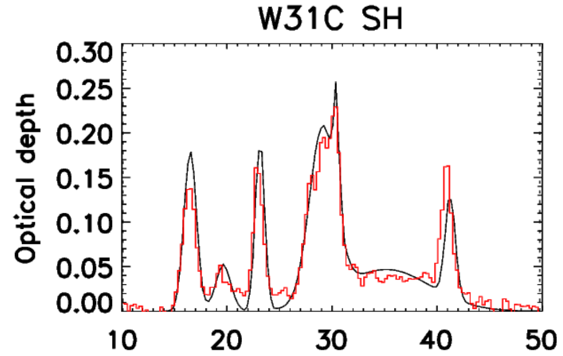

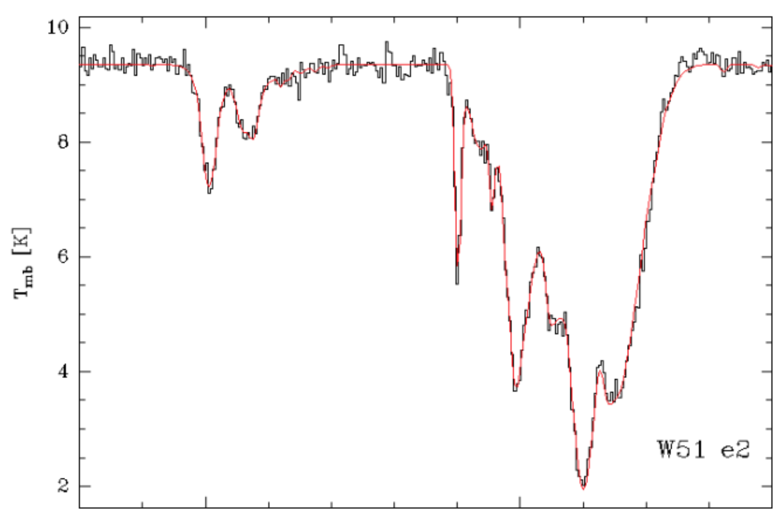

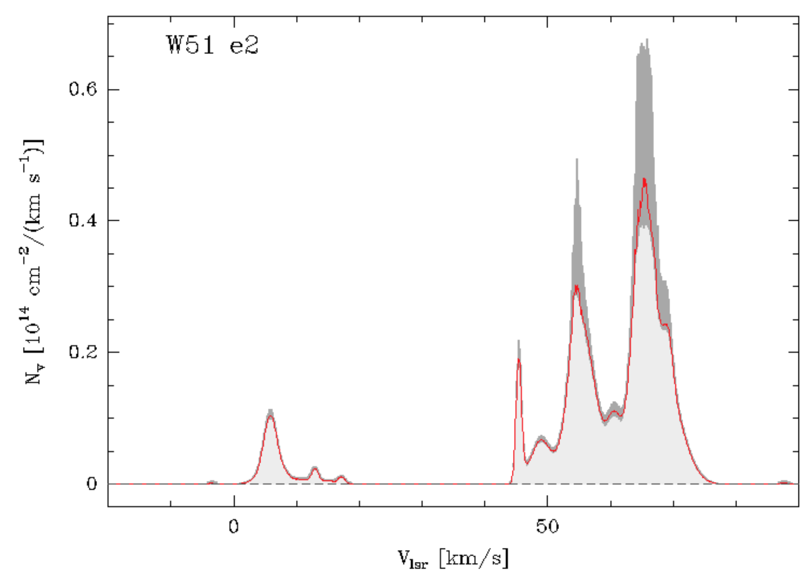

Left: observed CH $^2\Pi_{1.2}$ J = 3/2 ←1/2 spectru

Right: Deduced column density profile.

Correlations

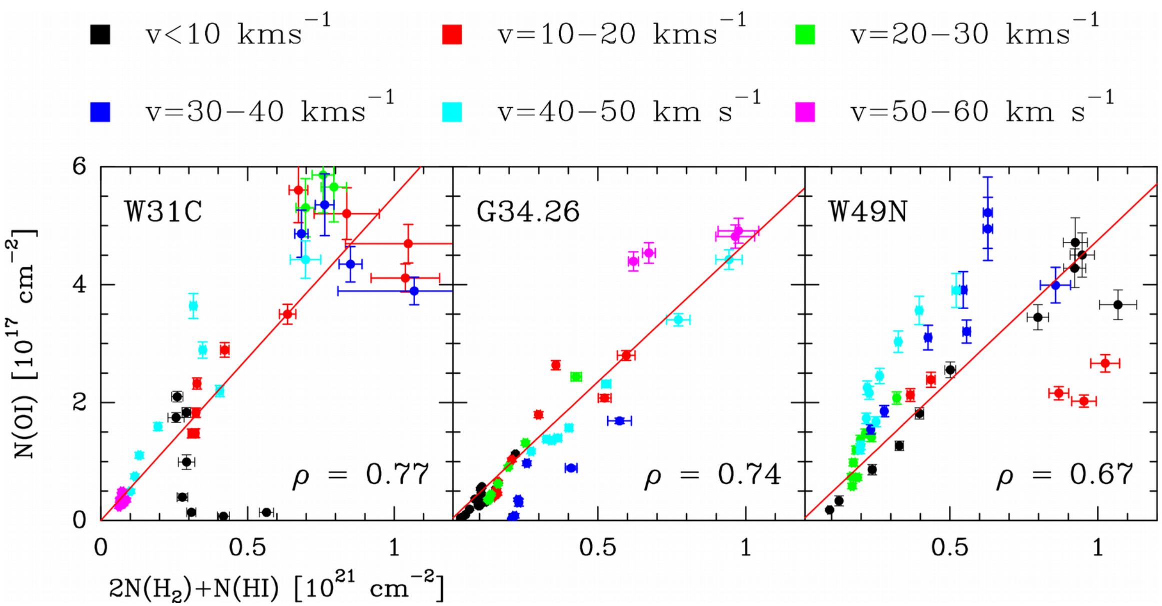

N(OI) vs. $2N(H_2)+N(HI)$
Wiesemeyer et al. 2016

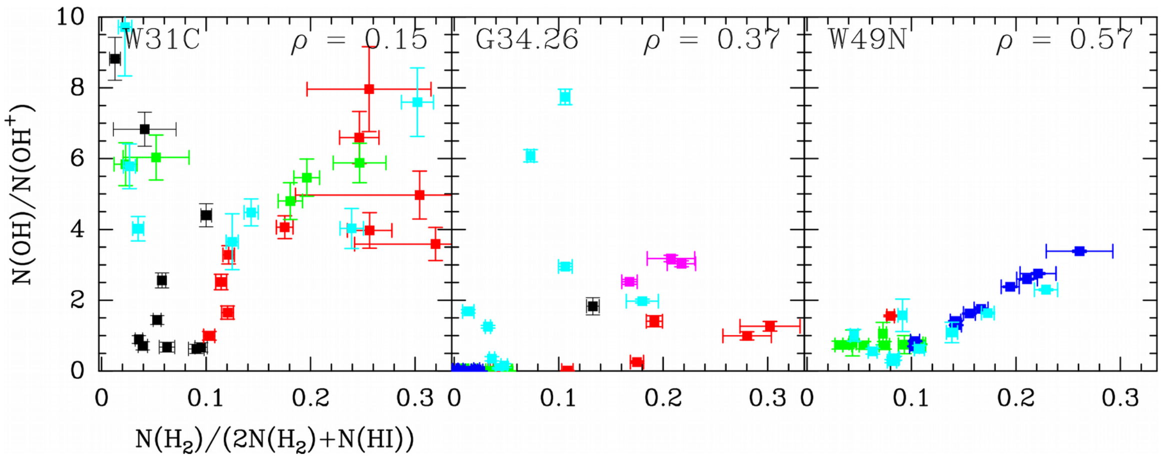

$N(OH)/N(OH^+)$ vs. f^N_{H2}
Wiesemeyer et al. 2016

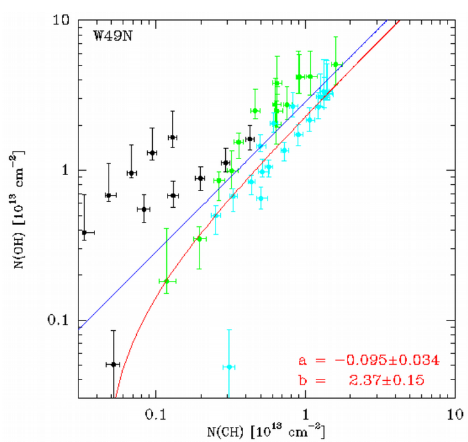

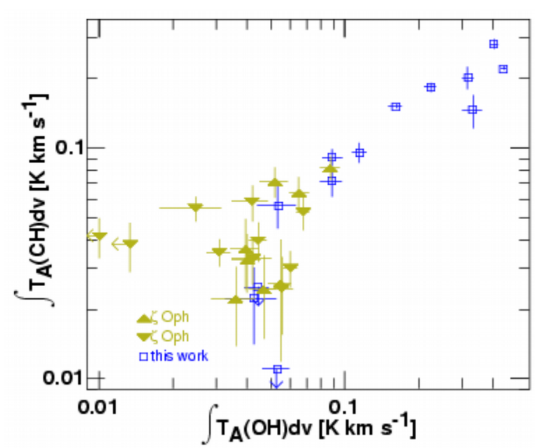

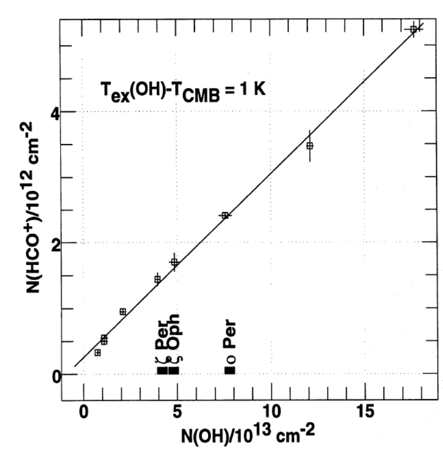

Left: CH vs OH
Wiesemeyer ea 2018
Liszt & Lucas 2002

Right: HCO^+ vs OH
Lucas & Liszt 1996

Dissociative recombinations

α $[10^{-10}\ s^{-1}]$ for T = 100 K,
$n_{e-} = 10^{-2}\ cm^{-3}$

OH^+	$+ e^-$	→	H	+ O	1.1
H_2O^+	$+ e^-$	→	H + H	+ O	52.8
		→	H	+ OH	14.9
		→	O	$+ H_2$	6.8
H_3O^+	$+ e^-$	→	H + H	+ OH	45.0
		→	H	$+ H_2O$	19.1
		→	H_2	+ OH	10.4
		→	H + O	$+ H_2$	1.0

Hydrogen abstraction reactions

α $[10^{-10}\ s^{-1}]$ for $n_{H2} = 10^2\ cm^{-3}$

OH^+	$+ H_2$	→	$H_2O^+ + H$	1100
H_2O^+	$+ H_2$	→	$H_3O^+ + H$	610

Photodissociation

α $[10^{-10}\ s^{-1}]$ for $A_v = 0.2$

OH^+	+ ν	→	$H^+ + O$	0.05
OH	+ ν	→	H + O	2.49
		→	$e^- + OH^+$	0.01
H_2O	+ ν	→	H + OH	5.15
		→	$e^- + H_2O^+$	0.14

Endothermic reactions & slow radiative association

O + H	→	γ + OH	< ~10^{-6}
O + H_2	→	H + OH	$6.34\ s^{-1}\ \exp(-4000/T[K])$
O(1D) + H_2	→	H + OH	103.
OH + H	→	H_2 + O	< ~ $0.001\ s^{-1}\ \exp(-1950/T[K])$
OH + H	→	γ + H_2O	< ~10^{-5}
OH + H_2	→	H + H_2O	$7.7\ s^{-1}\ \exp(-2100/T[K])$

Connection to C network

$OH + C^+ \rightarrow H + CO^+$

Source:

KIDA Database

Wakelam ea. 2012

/kida.obs.u-bordeaux1.fr

Meudon PDR Code Employed to Evaluate OH Abundance Under Different Conditions (credits to Paul Goldsmith)

- All runs have total extinction equal to 10 mag
- ISRF is standard Habing field (G_0 = 1) or 10x standard (G_0 = 10)
- Hydrogen nucleus density, n_H, is 50 cm^{-3} or 200 cm^{-3}
- Standard cosmic ray rates throughout; no enhanced rate at cloud edges as indicated by e.g. H_3^+ and other chemical tracers
- Standard grain properties
- Depleted sulfur abundance in accordance with most modeling

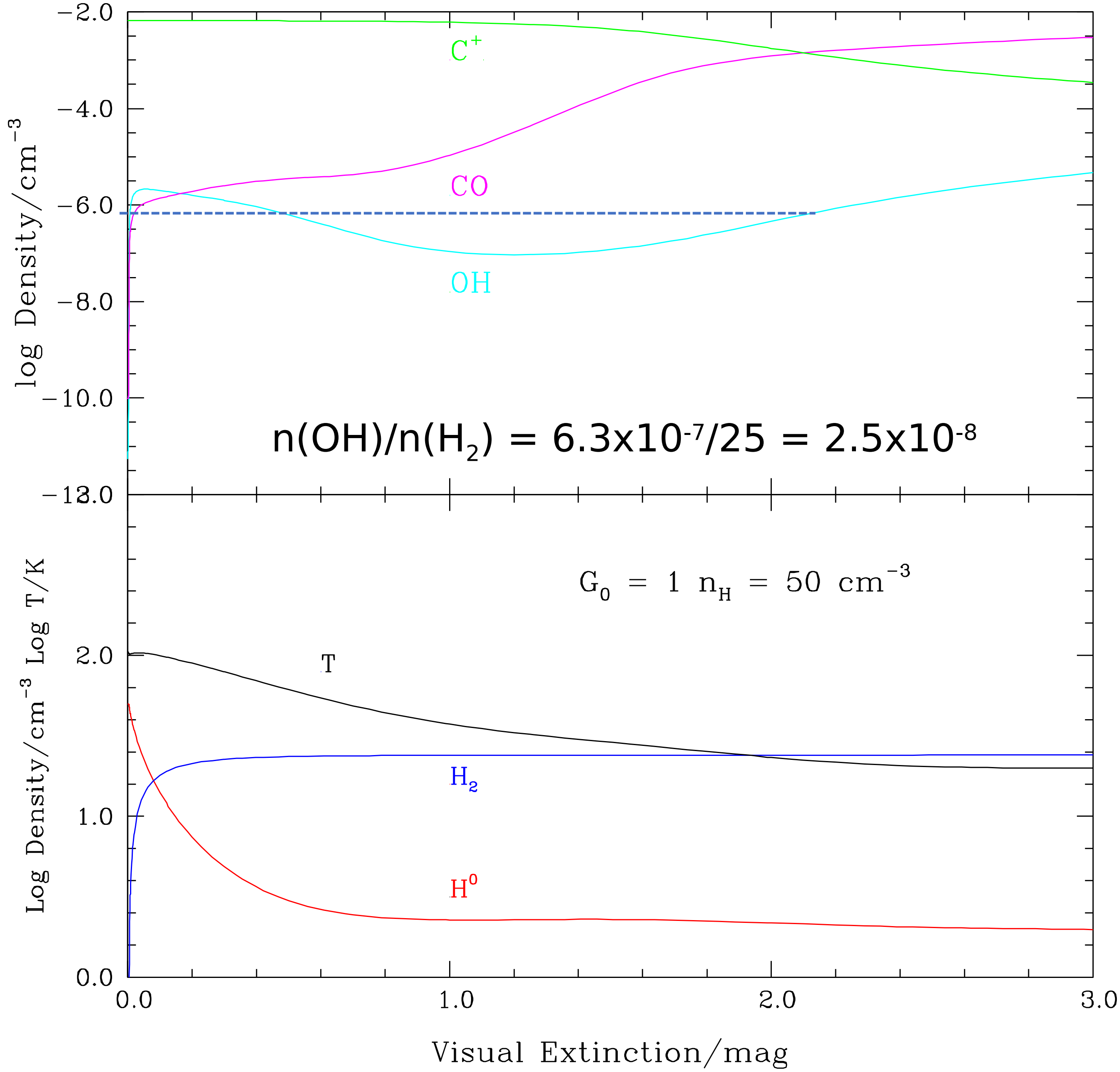

Key Aspects of Code Output

For standard ISRF, H-H_2 transition occurs at $A_v \sim 0.1$ mag:

hydrogen is largely atomic throughout T_k ~25 K for $A_v >$ 1mag (a little low) but rises to 200 K at cloud edge

C^+ is dominant form of carbon for $A_v < 2$ mag

X(CO) = 1.6×10^{-4} in interior of cloud but drops precipitously to ~8×10^{-8} for $A_v < 1$ mag

OH abundance relatively constant at 1.2×10^{-8} *THROUGHOUT* 0.05 mag $< A_v < 3$ mag

OH is a more unbiased tracer than CO throughout the region with $A_v < 3$ mag

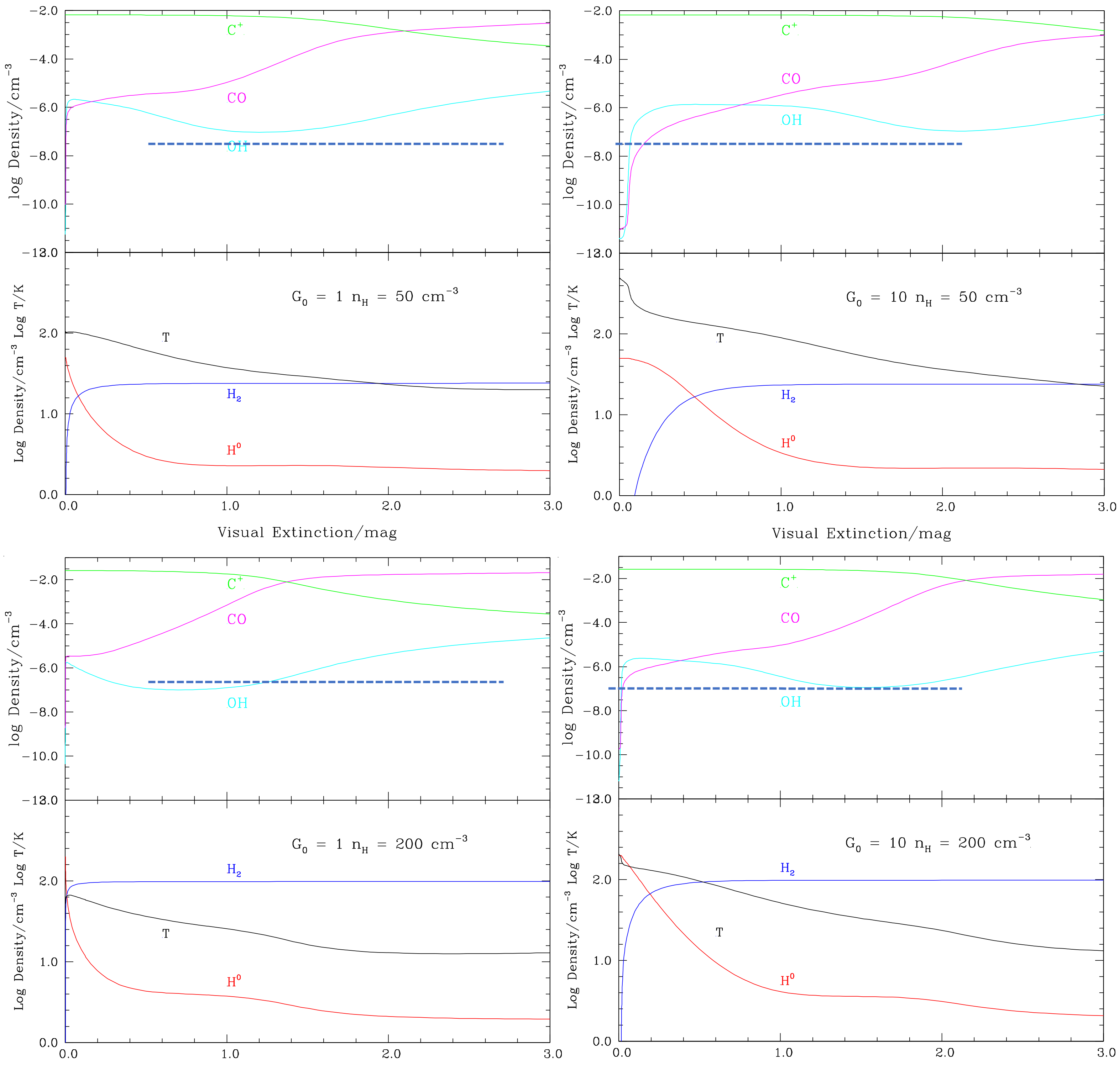

OH is a remarkably resilient tracer of total hydrogen nucleus density throughout the range $0 < A_V < 3$ mag, according to chemical modeling.

Larger G_0 heats cloud edge, thus increases OH formation rate but also increases the photodestruction rate.

No substantial variation, unlike CO which depends on self-shielding for protection against line photo-dissociation, and C^+ which disappears when CO builds up.

Higher density pushes H^0/H_2 transition to lower A_V, compensating the effect of higher G_0.

The case of CH – environmental diversity ?

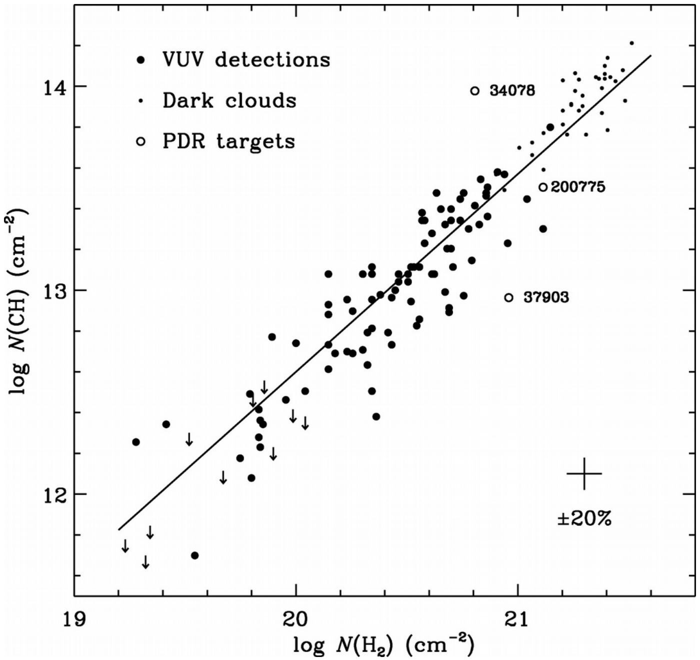

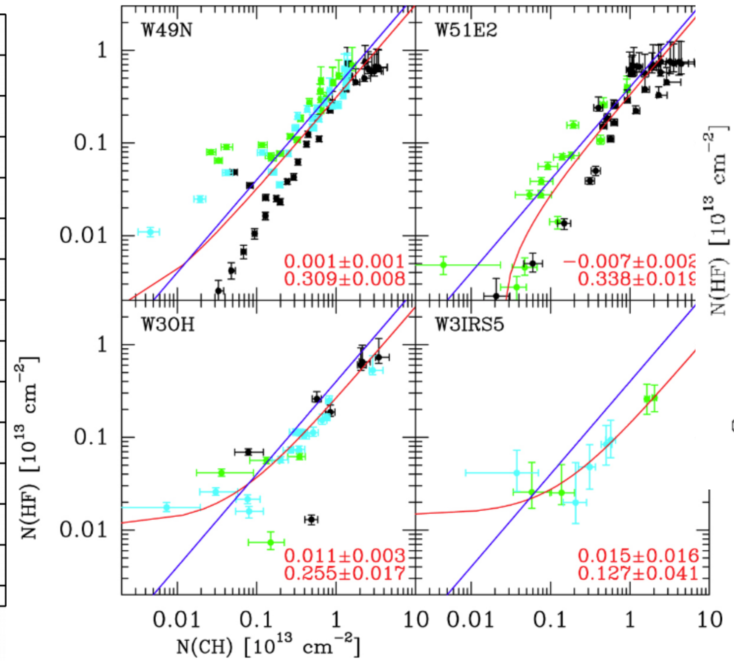

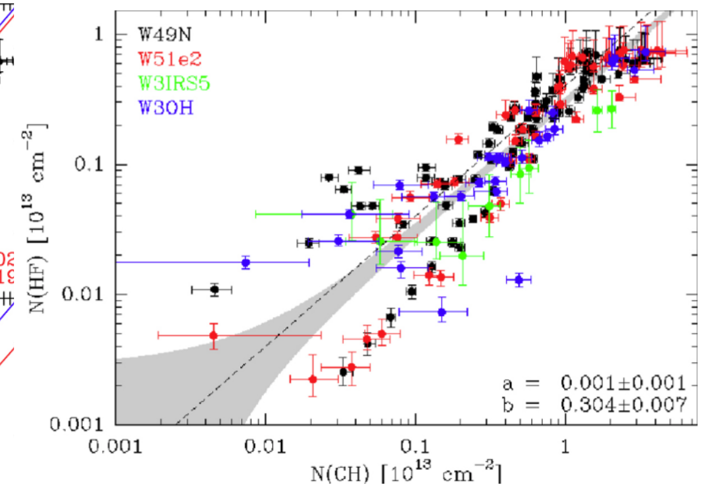

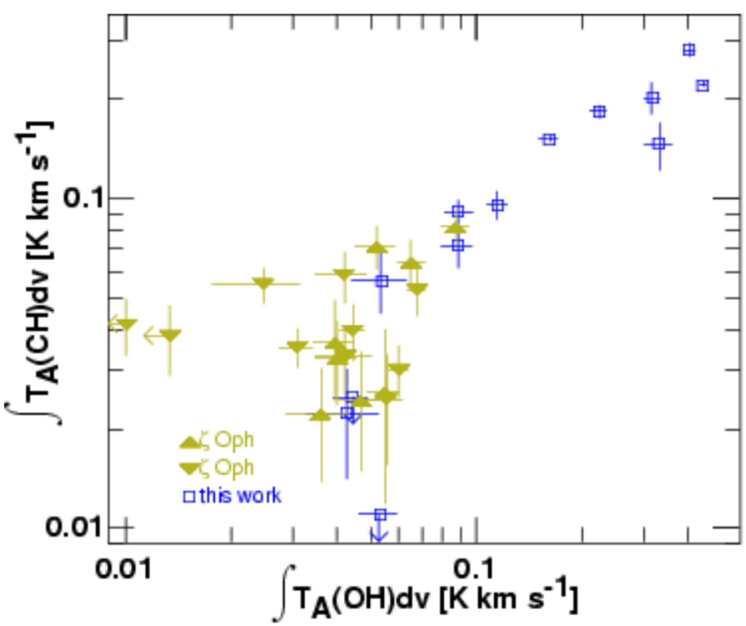

Top left: Sheffer et al. (2008, opt./UV), $N(CH)/N(H_2) = 3.5 \times 10^{-8}$

Top right: SOFIA/GREAT (Wiesemeyer et al. 2018) & PRISMAS (Gerin et al. 2012, Sonnentrucker et al 2015), four lines of sight & stacking analysis, overabundance of factor ~3 w.r.t. Sheffer et al. (2008)

Bottom left: Liszt & Lucas (2002)

Warm neutral-neutral chemistry

- The over-abundance of CH^+ (e.g., Elitzur & Watson 1978) is puzzling, due to the endothermicity of the key reaction $C^+(H_2,H)CH^+$ (4640 K).
- The dissipation of turbulence, C-type shocks, or ion-neutral friction can supply the activation energy (Godard ea 2014).
- This yields to an increased abundance of CH thanks to fast hydrogen abstraction reactions of CH^+ and the subsequent dissociative recombination of CH_3^+.
- OH and CH behave differently in quiescent and turbulent gas.

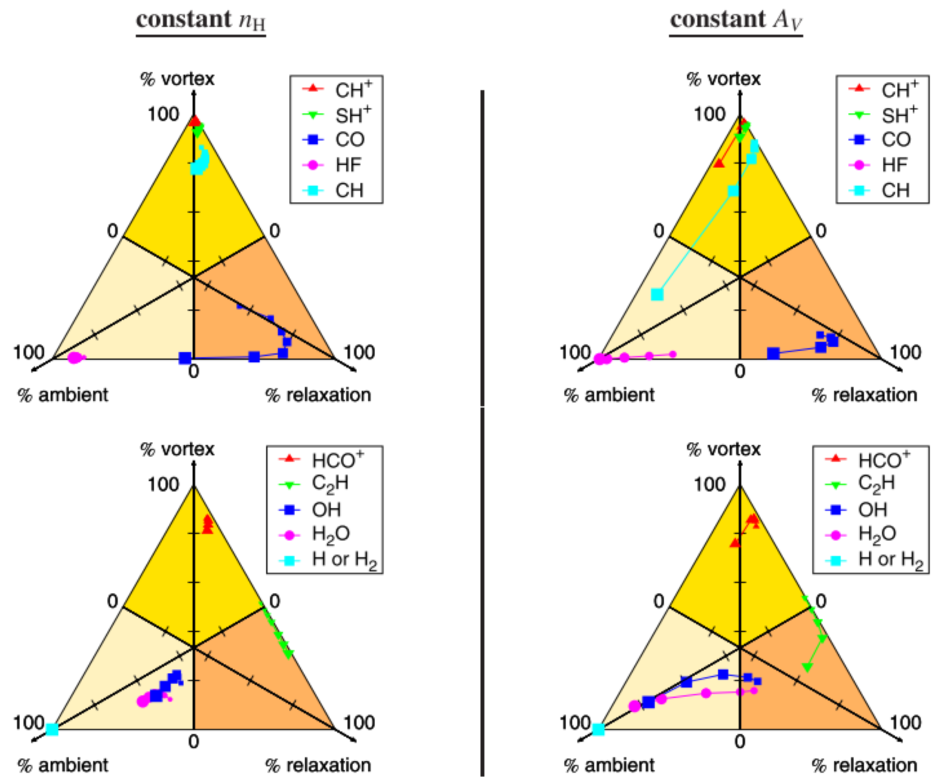

Phase diagrams of the TDR model (Godard et al. 2014)

Left: $n_H = 50$ cm^{-3}, $A_V = 0.1 - 1.0$ mag
Right: Av = 0.4 mag, $n_H = 20 - 300$ cm^{-3}

Towards more complexity – and reality ?

TDR model: Chemical enrichment due to endothermic reaction pathways only on a fraction of the sightline (Godard et al. 2014, Fig. 2) →

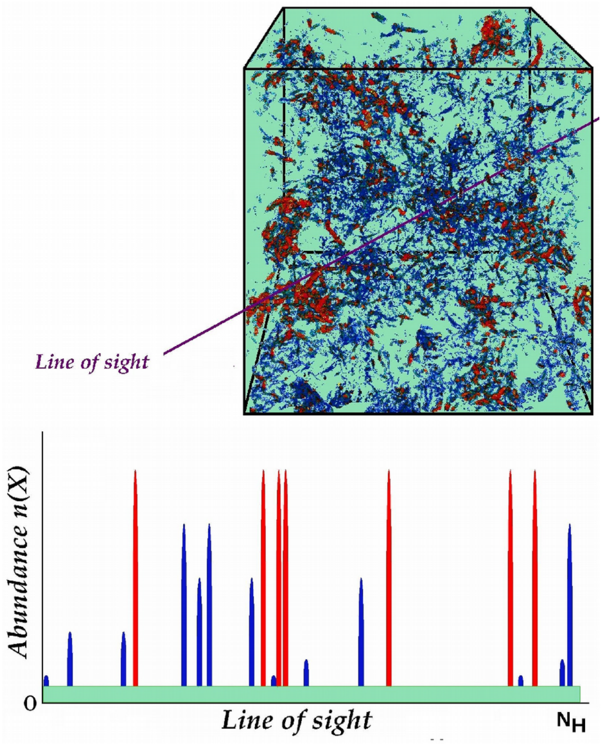

MHD simulations (Valdivia et al. 2017a,b) ↓

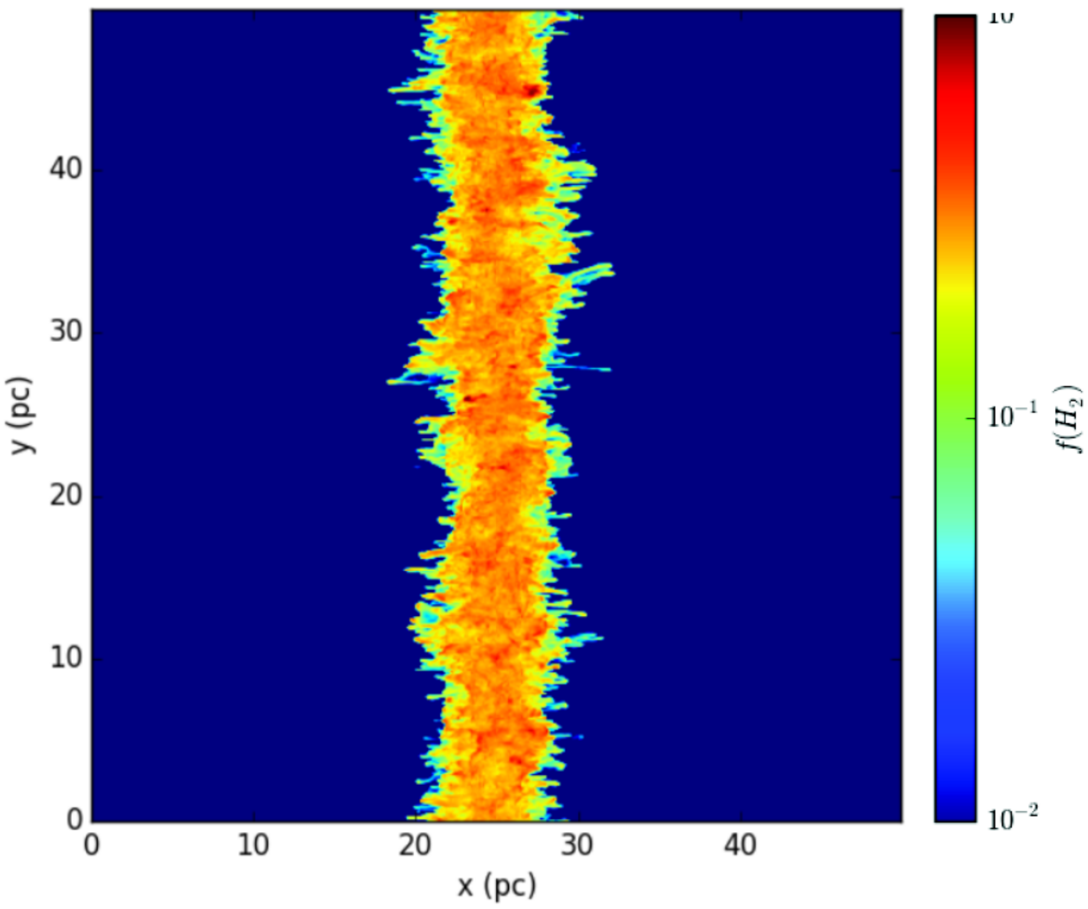

- Highly anisotropic A_V
- Ttransport of H_2 formed in UV shielded regions towards warmer regions where it triggers a warm chemistry.
- Magnetic fields slow down formation of denser structures, but also lead to more complexity.

Summary

The chemistry of the cold neutral medium, i.e., precursors of molecular clouds, is reasonably well understood.

Far-infrared spectroscopy with HIFI and SOFIA, completed with radio data, suggests that OH and CH are reliable surrogates for H_2 in CO-dark diffuse gas.

However, at low column densities CH tends to be over-abundant, presumably thanks to the endothermic production path of CH^+.

This observational evidence is confirmed by recent theoretical studies with a remarkable degree of complexity, assisted by experimental determinations of reaction rates at a relevant range of temperatures.

Caveat: Spectral features, even at the velocity of a single spiral arm crossing, do not necessarily represent a single cloud entity, but rather a weighted average of a complex medium.